



IMPLEMENTING MULTI-SCALE AGRICULTURAL INDICATORS EXPLOITING SENTINELS

**VEGETATION FIELD DATA AND PRODUCTION OF
GROUND-BASED MAPS:**

**“PSHENICHNE SITE, UKRAINE”
12TH JUNE, 31ST JULY 2014**

ISSUE I1.00

EC Proposal Reference N° FP7-311766

Actual submission date : April 2015

Start date of project: 01.11.2012

Duration : 40 months



Name of lead partner for this deliverable: EOLAB

Book Captain: Consuelo Latorre (EOLAB)

Contributing Authors: María del Carmen Piñó (EOLAB), Fernando Camacho (EOLAB),
Nataliia Kussul, Serhiy Skakun, Andrii Kolotii, Andrii Shelestov
(NAS-SSAU)

Project co-funded by the European Commission within the Seventh Framework Program (2007-2013)		
Dissemination Level		
PU	Public	X
PP	Restricted to other programme participants (including the Commission Services)	
RE	Restricted to a group specified by the consortium (including the Commission Services)	
CO	Confidential, only for members of the consortium (including the Commission Services)	

DOCUMENT RELEASE SHEET

Book Captain:	Consuelo Latorre	Date: 01.04.2015	Sign. 
Approval:	R. Lacaze	Date: 17.06.2015	Sign. 
Endorsement:	I. Marin-Moreno	Date:	Sign.
Distribution:			

CHANGE RECORD

Issue/Revision	Date	Page(s)	Description of Change	Release
	01.04.2015	All	First Issue	I1.00

TABLE OF CONTENTS

1.	<i>Background of the Document</i>	10
1.1.	Executive Summary	10
1.2.	Portfolio	10
1.3.	Scope and Objectives.....	11
1.4.	Content of the Document	11
1.5.	Related Document.....	11
2.	<i>Introduction</i>	12
3.	<i>Study area</i>	13
3.1.	Location	13
3.2.	Description of The Test Site	13
4.	<i>Ground MEASUREMENTS</i>	15
4.1.	Material and Methods	15
4.2.	Spatial Sampling Scheme	16
4.3.	ground data.....	18
4.3.1.	Data processing	18
4.3.2.	Content of the Ground Dataset.....	19
5.	<i>Evaluation of the sampling</i>	22
5.1.	Evaluation Based On NDVI Values.....	22
5.2.	Evaluation Based On Convex Hull: Product Quality Flag.	23
6.	<i>Production of ground-based maps</i>	25
6.1.	Imagery	25
6.2.	The Transfer Function.....	26
6.2.1.	The regression method.....	26
6.2.2.	Band combination	27
6.2.3.	The selected Transfer Function	28
6.3.	The High Resolution Ground Based Maps	30
6.3.1.	Mean Values	33
7.	<i>Conclusions</i>	35
8.	<i>Acknowledgements</i>	36
9.	<i>References</i>	37

LIST OF FIGURES

Figure 1: Location of Pshenichne site, Ukraine.....	13
Figure 2: Land cover types sampled and the location of the ESUs over the Pshenichne site, 12 th June, 2014.	14
Figure 3: False color composition (RGB: SWIR-NIR-Red) of TOA image over the 20x20 km ² study area Pshenichne, Ukraine, 2014. Left: Landsat-8 (12 th , June). Right: Landsat-7 (31 st , July).....	14
Figure 4: Distribution of the sampling units (ESUS) over the study area. Orange points: First campaign (12 th June, 2014). Red points: Second campaign (31 st July, 2014). Pshenichne, Ukraine.....	17
Figure 5: ESU land cover distribution of Pshenichne-Ukraine. Left side: First campaign (12 th June, 2014). Right side: Second campaign (31 st July, 2014).....	17
Figure 6: Inter-comparison of the measured biophysical variables. LAI versus FAPAR (Left) and FAPAR versus FCOVER (Right). Pshenichne, Ukraine 12 th June, 2014.	18
Figure 7: Inter-comparison of the measured biophysical variables. LAI versus FAPAR (Left) and FAPAR versus FCOVER (Right). Pshenichne, Ukraine 31 st July, 2014.....	18
Figure 8: LAI _{eff} and LAI measurements by land cover type over Pshenichne site, Ukraine. Left: 12 th June. Right: 31 st July.....	19
Figure 9: FAPAR measurements by land cover type over Pshenichne site, Ukraine. Left: 12 th June. Right: 31 st July.	20
Figure 10: FCOVER measurements by land cover type over Pshenichne site, Ukraine. Left: 12 th June. Right: 31 st July.	20
Figure 11: Distribution of the measured biophysical variables. Left side: First campaign. Right side: Second campaign.	20
Figure 12: Comparison of NDVI distribution between ESUs and over the whole image, Pshenichne-Ukraine, 2014. Left: 12 th June, 2014 Right: 31 st July, 2014.....	22
Figure 13: Convex Hull test over 20x20 km ² and 5x5 km ² areas over Pshenichne site, Ukraine. Left side: 12 th June, 2014. Right side: 31 st July, 2014. Clear and dark blue correspond to the pixels belonging to the 'strict' and 'large' convex hulls. Red corresponds to the pixels for which the transfer function behaves as extrapolator.....	24
Figure 14: Landsat-8 image for one proximal date (left), the original image Landsat-7 with gaps (middle) and the restored image using the NSPI method (right). Example for NIR bands (B4 for Landsat-7 and B5 for Landsat-8).....	25
Figure 15: Vertical profile over the Pshenichne site, for NIR band of original Landsat-7 image (Left) and gap filled Landsat-7 image (Right).....	25
Figure 16: Test of multiple regression (TF) applied on different band combinations. Band combinations are given in abscissa (1=G, 2=RED, 3=NIR and 4=SWIR). The weighted root mean square error (RMSE) is presented in red along with the cross-validation RMSE in green. The numbers indicate the number of data used for the robust regression with a weight lower than 0.7 that could be considered as outliers. Left side: 12 th June, 2014. Right side: 31 st July, 2014.	27
Figure 17: LAI _{eff} , LAI, FAPAR and FCOVER results for regression on reflectance using 4 bands combination. Full dots: Weight>0.7. Empty dots: 0<Weight<0.7.	29
Figure 18: High resolution biophysical LAI _{eff} maps applied on the Pshenichne site. Left: 12 th June, 2014. Right: 31 st July, 2014.....	30
Figure 19: High resolution biophysical LAI maps applied on the Pshenichne site. Left: 12 th June, 2014. Right: 31 st July, 2014.	30
Figure 20: High resolution biophysical FAPAR maps applied on the Pshenichne site. Left: 12 th June, 2014. Right: 31 st July, 2014.....	31

Figure 21: High resolution biophysical FCOVER maps applied on the Pshenichne site. Left: Pshenichne-Ukraine (12th June, 2014). Right: Pshenichne-Ukraine (31st July, 2014)..... 31

Figure 22: Ground-based maps (5x5 km²) retrieved on the Pshenichne site. Left: First campaign. Right: Second campaign. 32

Figure 23: Scatter plots to LAI vs FAPAR and FAPAR vs FCOVER for the two campaigns over Pshenichne-Ukraine. Right: 12th June, 2014. Left: 31st July, 2014. 33

LIST OF TABLES

<i>Table 1: Coordinates and altitude of the test site (centre).....</i>	<i>13</i>
<i>Table 2: Distribution of land cover types sampled in Pshenichne, 2014.</i>	<i>17</i>
<i>Table 3: The Header used to describe ESUs with the ground measurements.</i>	<i>19</i>
<i>Table 4: Percentages over the two areas over the test site of Pshenichne (Ukraine) Convex hull values: 0=extrapolation of TF, 1=strict convex hull and 2=large convex hull).</i>	<i>23</i>
<i>Table 5: Acquisition properties of Landsat-8 and Landsat-7 data used for retrieving high resolution maps.....</i>	<i>26</i>
<i>Table 6: Transfer function applied to the whole site for LAIeff, LAI, FAPAR daily integrated and FCOVER. RW for weighted RMSE, and RC for cross-validation RMSE</i>	<i>28</i>
<i>Table 7: Mean values and standard deviation (STD) of the HR biophysical maps for the selected 3 x 3 km2 area at Pshenichne site (Ukraine).....</i>	<i>34</i>
<i>Table 8: Content of the dataset.....</i>	<i>34</i>

LIST OF ACRONYMS

CEOS	Committee on Earth Observation Satellite
CEOS LPV	Land Product Validation Subgroup
CNR	<i>Consiglio Nazionale delle Ricerche</i>
DG AGRI	Directorate General for Agriculture and Rural Development
DG RELEX	Directorate General for External Relations (European Commission)
DHP	Digital Hemispheric Photographs
ECV	Essential Climate Variables
EUROSTATS	Directorate General of the European Commission
ERMES	An Earth Observation Model based Rice Information Service
ESU	Elementary Sample Unit
FAPAR	Fraction of Absorbed Photo-synthetically Active Radiation
FAO	Food and Agriculture Organization
FCOVER	Fraction of Vegetation Cover
GCOS	Global Climate Observing System
GEO-GLAM	Global Agricultural Geo- Monitoring Initiative
GIO-GL	GMES Initial Operations - Global Land (GMES)
GCOS	Global Climate Observing System
GMES	Global Monitoring for Environment and Security
GPS	Global Positioning System
IMAGINES	Implementing Multi-scale Agricultural Indicators Exploiting Sentinels
JECAM	Joint Experiment for Crop Assessment and Monitoring
LAI	Leaf Area Index
LDAS	Land Data Assimilation System
LUT	Look-up-table techniques
NSPI	Neighborhood Similar Pixel Interpolator
PAI	Plant Area Index
PROBA-V	Project for On-Board Autonomy satellite, the V standing for vegetation.
RMSE	Root Mean Square Error
SPOT /VGT	Satellite Pour l'Observation de la Terre / VEGETATION
SLT	Solar Local Time
TOC	Top of Canopy Reflectance
USGS	U.S. Geological Survey. Science organization.
UNFCCC	United Nations Framework Convention on Climate Change
UTM	Universal Transverse Mercator coordinates system
VALERI	Validation of Land European Remote sensing Instruments
WGCV	Working Group on Calibration and Validation (CEOS)

1. BACKGROUND OF THE DOCUMENT

1.1. EXECUTIVE SUMMARY

The Copernicus Land Service has been built in the framework of the FP7 geoland2 project, which has set up pre-operational infrastructures. ImagineS intends to ensure the continuity of the innovation and development activities of geoland2 to support the operations of the global land component of the GMES Initial Operation (GIO) phase. In particular, the use of the future Sentinel data in an operational context will be prepared. Moreover, IMAGINES will favor the emergence of new downstream activities dedicated to the monitoring of crop and fodder production.

The main objectives of ImagineS are to (i) improve the retrieval of basic biophysical variables, mainly LAI, FAPAR and the surface albedo, identified as Terrestrial Essential Climate Variables, by merging the information coming from different sensors (PROBA-V and Landsat-8) in view to prepare the use of Sentinel missions data; (ii) develop qualified software able to process multi-sensor data at the global scale on a fully automatic basis; (iii) complement and contribute to the existing or future agricultural services by providing new data streams relying upon an original method to assess the above-ground biomass, based on the assimilation of satellite products in a Land Data Assimilation System (LDAS) in order to monitor the crop/fodder biomass production together with the carbon and water fluxes; (iv) demonstrate the added value of this contribution for a community of users acting at global, European, national, and regional scales.

Further, ImagineS will serve the growing needs of international (e.g. FAO and NGOs), European (e.g. DG AGRI, EUROSTATS, DG RELEX), and national users (e.g. national services in agro-meteorology, ministries, group of producers, traders) on accurate and reliable information for the implementation of the EU Common Agricultural Policy, of the food security policy, for early warning systems, and trading issues. ImagineS will also contribute to the Global Agricultural Geo-Monitoring Initiative (GEO-GLAM) by its original agriculture service which can monitor crop and fodder production together with the carbon and water fluxes and can provide drought indicators, and through links with JECAM (Joint Experiment for Crop Assessment and Monitoring).

1.2. PORTFOLIO

The ImagineS portfolio contains global and regional biophysical variables derived from multi-sensor satellite data, at different spatial resolutions, together with agricultural indicators, including the above-ground biomass, the carbon and water fluxes, and drought indices resulting from the assimilation of the biophysical variables in the Land Data Assimilation System (LDAS).

The production in Near Real Time of the 333m resolution products, at a frequency of 10 days, using PROBA-V data will be carried out in the Copernicus Global Land Service. It should start by covering Europe only, and be gradually extended to the whole globe.

Meanwhile, ImagineS will perform in parallel off-line production over demonstration sites outside Europe. The demonstration of high resolution (30m) products (Landsat-8 + PROBA-

V) will be done over demonstration sites of cropland and grassland in contrasting climatic and environmental conditions.

1.3. SCOPE AND OBJECTIVES

The main objective of this document is to describe the ground database provided by the Space Research Institute NAS and SSA Ukraine, and the processing carried out by EOLAB to derive high resolution maps of the following biophysical variables:

- Leaf Area Index (LAI), defined as half of the total developed area of leaves per unit ground surface area (m^2/m^2). We focused on two different LAI quantities (for green elements):
 - The effective LAI (LAI_{eff}) derived from the description of the gap fraction as a function of the view zenith angle. In addition, effective LAI measures derived at 57.5° are also provided in the ground database.
 - The actual LAI (LAI) estimate corrected from the clumping index.
- Fraction of green Vegetation Cover (FCover), defined as the proportion of soil covered by vegetation, derived from the gap fraction between 0 and 10° of view zenith angle.
- Fraction of Absorbed Photosynthetically Active Radiation (FAPAR), which is the fraction of the photosynthetically active radiation (PAR) absorbed by a vegetation canopy. We are also focused on green elements. PAR is the solar radiation reaching the canopy in the $0.4\text{--}0.7\ \mu\text{m}$ wavelength region. We focused on the daily integrated FAPAR computed as the black-sky FAPAR integrated over the day.

1.4. CONTENT OF THE DOCUMENT

This document is structured as follows:

- Chapter 2 provides an introduction to the field experiment.
- Chapter 3 provides the location and description of the site.
- Chapter 4 describes the ground measurements, including material and methods, sampling and data processing.
- Chapter 5 provides an evaluation of the sampling.
- Chapter 6 describes the production of high resolution ground-based maps, and the selected “mean” values for validation.

1.5. RELATED DOCUMENT

ImagineS_RP7.5_FieldCampaign_Pshenichne2013: Field campaign and Data Processing report of the measurements collected in 2013 over Pshenichne site.

2. INTRODUCTION

Validation of remote sensing products is mandatory to guaranty that the satellite products meets the user's requirements. Protocols for validation of global LAI products are already developed in the context of Land Product Validation (LPV) group of the Committee on Earth Observation Satellite (CEOS) for the validation of satellite-derived land products (Fernandes et al., 2014), and recently applied to Copernicus global land products based on SPOT/VGT observation (Camacho et al., 2013). This generic approach is made of 2 major components:

- The indirect validation: including inter-comparison between products as well as evaluation of their temporal and spatial consistency
- The direct validation: comparing satellite products to ground measurements of the corresponding biophysical variables. In the case of low and medium resolution sensors, the main difficulty relies on scaling local ground measurements to the extent corresponding to pixels size. However, the direct validation is limited by the small number of sites, for that reason a main objective of ImagineS is the collection of ground truth data in demonstration sites.

The content of this document is compliant with existing validation guidelines (for direct validation) as proposed by the CEOS LPV group (Morissette et al., 2006); the VALERI project (<http://w3.avignon.inra.fr/valeri/>) and ESA campaigns (Baret and Fernandes, 2012). It therefore follows the general strategy based on a bottom up approach: it starts from the scale of the individual measurements that are aggregated over an elementary sampling unit (ESU) corresponding to a support area consistent with that of the high resolution imagery used for the up-scaling of ground data. Several ESUs are sampled over the site. Radiometric values over a decametric image are also extracted over the ESUs. This will be later used to develop empirical transfer functions for up-scaling the ESU ground measurements (e.g. Martínez et al., 2009). Finally, the high resolution ground based map will be compared with the medium resolution satellite product at the spatial support of the product.

One of the Imagines demonstration sites selected to support the validation of Copernicus Global Land is located in Pshenichne, Ukraine. In the framework of JECAM (Joint Experiment for Crop Assessment and Monitoring) initiative, the Space Research Institute NAS and SSA Ukraine has carried out two campaigns to characterize the vegetation biophysical parameters at the test site of Pshenichne.

First Campaign: 12th of June 2014.

Second Campaign: 31st of July 2014

Teams involved in field collection: Natalia Kussul, Skakun Serhiy, Kravchenko Oleksiy

Contact: Natalia Kussul (kussul@mail.ru)

3. STUDY AREA

3.1. LOCATION

The experimental site is located around Pshenichne farm, in the region of Kiev, 50 km away from the capital (Figure 1). Ground measurements were conducted over selected fields located on the side of Pshenichne. The coordinates of the test site have shown in the Table 1.

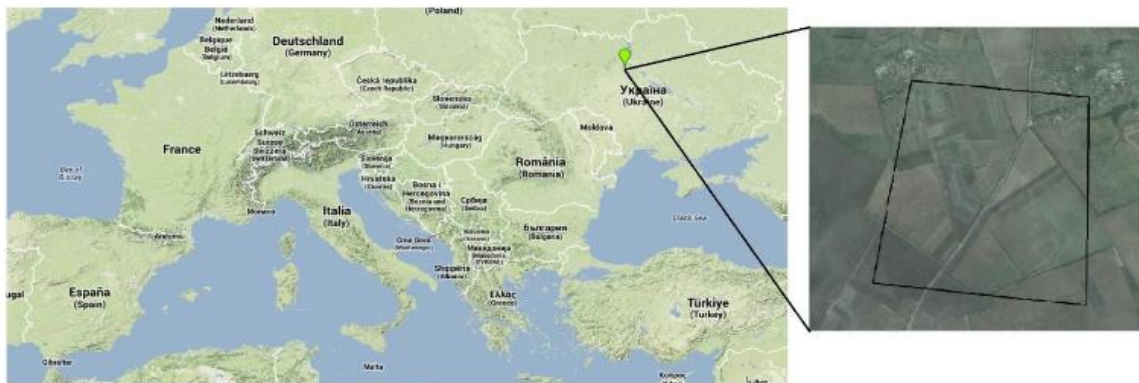


Figure 1: Location of Pshenichne site, Ukraine.

Table 1: Coordinates and altitude of the test site (centre).

Site Center	
Geographic Lat/Ion, WGS-84 (degrees)	Latitude = 50.0765' E Longitude = 30.2322' N
Altitude	200 m

3.2. DESCRIPTION OF THE TEST SITE

Crop types in the region of Pshenichne are typically winter wheat, spring barley, maize, soy beans, winter rapeseed, sunflower, sugar beet, potatoes, winter rye, and spring wheat (see Figure 2). There is not a typical simple crop rotation in this region. Most producers use different crop rotations depending on specialization.

4. GROUND MEASUREMENTS

The ground data measurement database was acquired and provided by the Space Research Institute NAS Ukraine and SSA Ukraine.

4.1. MATERIAL AND METHODS

Digital Hemispherical Photographs (DHP) were acquired with a NIKON D70 camera. Hemispherical photos allow the calculation of LAI and FCOVER measuring gap fraction through an extreme wide-angle camera lens (i.e. 180°) (Weiss et al; 2004). It produces circular images that record the size, shape, and location of gaps, either looking upward from within a canopy or looking downward from above the canopy.

The hemispherical images acquired during the field campaign are processed with the CAN-EYE software (http://www.avignon.inra.fr/can_eye) to derive LAI, FAPAR and FCOVER. It is based on a RGB color classification of the image to discriminate vegetation elements from background (i.e., gaps). This approach allows exploiting downward-looking photographs for short canopies (background = soil) as well as upward-looking photographs for tall canopies (background = sky). CAN-EYE software processes simultaneously up to of N = 16 images acquired over the same ESU. Note that the N images were acquired with similar illumination conditions to limit the variation of colour dynamics between images.

The CAN-EYE software computes biophysical variables from gap fraction as follows:

Effective LAI (LAI_{eff}) is computed from the gap fraction P_0 , CAN-EYE(θ) following the Poisson law (Welles and Norman, 1991):

$$P_{0,CANEYE}(\theta) = \frac{e^{-L_{eff}G(\theta,\varphi,\theta_{leaf,eff})}}{\cos\theta} \quad \text{Eq. (1)}$$

Where θ and φ are respectively the zenith and azimuth angles of the direction of propagation of the incident beam, L_{eff} refers to effective LAI, G is the mean projection of a leaf area unit in a plane perpendicular to direction (θ,φ) which is directly dependent of the leaf angle distribution for the inclination. It is thus fully characterized with the average leaf angle (ALA) only. Two variables are therefore needed to describe canopy architecture under these assumptions: the effective LAI (L_{eff}) and effective ALA ($\theta_{leaf,eff}$). A look-up-table (LUT) is used to estimate L_{eff} and $\theta_{leaf,eff}$ from the measured zenithal variation of the gap fraction (Weiss et al., 2004).

LAI: The actual LAI that can be measured only with a planimeter with however possible allometric relationships to reduce the sampling, is related to the effective leaf area index through:

$$LAI_{eff} = \lambda_0 \cdot LAI \quad \text{Eq. (2)}$$

where λ_0 is the clumping index. In CAN-EYE, the clumping index is computed using the Lang and Xiang (1986) logarithm gap fraction averaging method, although some uncertainties are associated to this method (Demarez et al., 2008). The principle is based on the assumption that vegetation elements are locally assumed randomly distributed. Values of clumping index given by CAN_EYE are in certain cases correlated with the size of the cells used to divide photographs.

FCOVER is retrieved from gap fraction between 0 to 10°.

$$FCOVER = 1 - P_0 \cdot (0 - 10^\circ) \quad \text{Eq. (3)}$$

FAPAR: As there is little scattering by leaves in that particular spectral domain due to the strong absorbing features of the photosynthetic pigments, FAPAR is often assumed to be equal to FIPAR (Fraction of Intercepted Photosynthetically Active Radiation), and therefore directly related to the gap fraction. The actual FAPAR is the sum of two terms, weighted by the diffuse fraction in the PAR domain: the ‘black sky’ FAPAR that corresponds to the direct component and the ‘white sky’ or the diffuse component.

The instantaneous “Black-sky FAPAR” ($FAPAR^{BS}$) is given at a solar position (date, hour and latitude). Depending on latitude, the CAN EYE software computes the solar zenith angle every solar hour during half the day (there is symmetry at 12:00). The instantaneous FAPAR is then approximated at each solar hour as 1 minus the gap fraction in the corresponding solar zenith angle:

$$FAPAR^{BS}(\theta_S) = 1 - P_0 \cdot (\theta_S) \quad \text{Eq. (4)}$$

The daily integrated black sky or direct FAPAR is computed as the following:

$$FAPAR_{Day}^{BS} = \frac{\int_{sunset}^{sunrise} \cos(\theta_S) \cdot [1 - P_0 \cdot (\theta_S)] \cdot d\theta}{\int_{sunset}^{sunrise} \cos(\theta_S) \cdot d\theta} \quad \text{Eq. (5)}$$

4.2. SPATIAL SAMPLING SCHEME

A total of 28 ESUs in the first campaign were characterized and 25 ESUs during the second one (Table 2). A pseudo-regular sampling was used within each ESU of approximately 30x30 m². The centre of the ESU was geo-located using a Global Positioning System (GPS). Six different land cover types were characterized during the first campaign and five during the second campaign, the predominant crop sampled was Maize (>50% of the samples) (see Figure 5).

The sampling scheme for the different campaigns is shown in Figure 4.

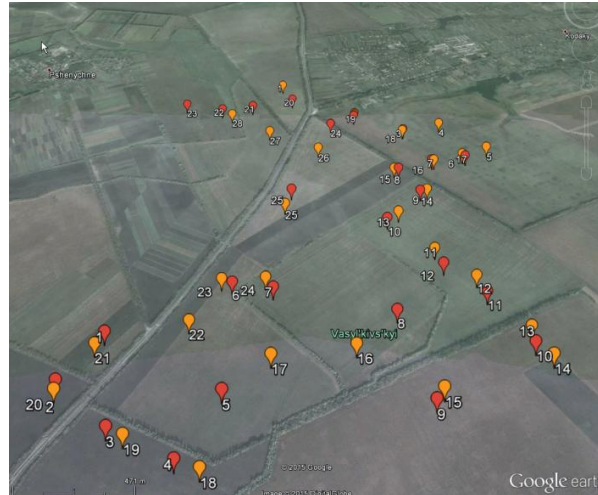


Figure 4: Distribution of the sampling units (ESUS) over the study area. Orange points: First campaign (12th June, 2014). Red points: Second campaign (31st July, 2014). Pshenichne, Ukraine

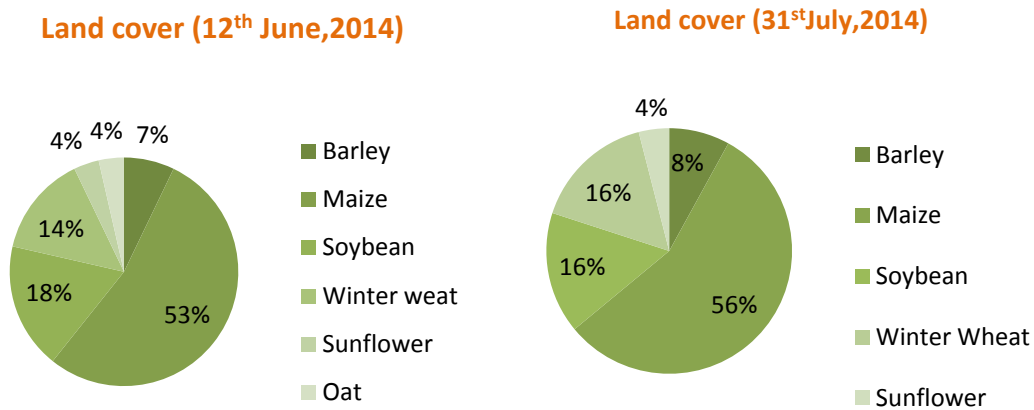


Figure 5: ESU land cover distribution of Pshenichne-Ukraine. Left side: First campaign (12th June, 2014). Right side: Second campaign (31st July, 2014).

Table 2: Distribution of land cover types sampled in Pshenichne, 2014.

Land Use	Number of ESUs	
	First campaign	Second campaign
Barley	2	2
Maize	15	14
Soybean	5	4
Oat	1	0
Winter wheat	4	4
Sunflower	1	1
Total of ESUs	28	25

4.3. GROUND DATA

4.3.1. Data processing

Figure 6 and Figure 7 shows the inter-comparison between LAI and LA_{eff} with FAPAR estimates, and between FAPAR and FCOVER for both campaigns. As can be observed, the relationship between variables follows an exponential trend between LAI and FAPAR, and a linear trend between FCOVER and FAPAR, as expected. Note that there are some dispersion between FAPAR and FCOVER in the first campaign.

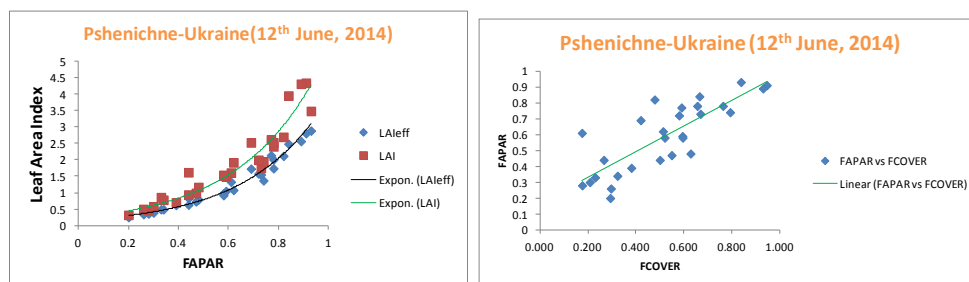


Figure 6: Inter-comparison of the measured biophysical variables. LAI versus FAPAR (Left) and FAPAR versus FCOVER (Right). Pshenichne, Ukraine 12th June, 2014.

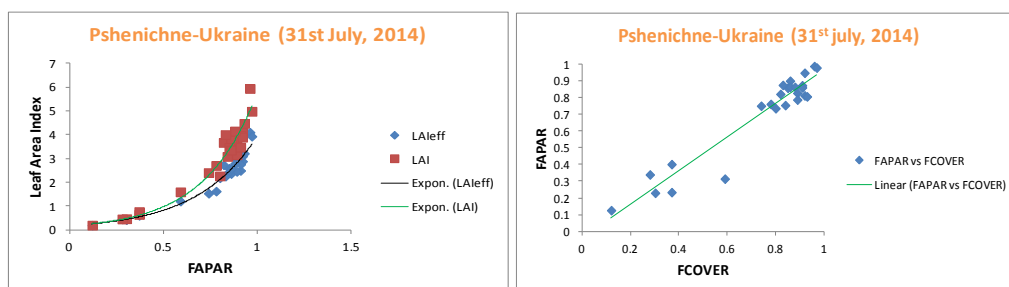


Figure 7: Inter-comparison of the measured biophysical variables. LAI versus FAPAR (Left) and FAPAR versus FCOVER (Right). Pshenichne, Ukraine 31st July, 2014.

In the second campaign, can be observed exponential trend between LAI and FAPAR and linear trend between FAPAR and FCOVER. In this campaign, the points are less scattered than the first campaign (Figure 6, Right).

4.3.2. Content of the Ground Dataset

Each ESU is described according to a standard format. The header of the database is shown in Table 3.

Table 3: The Header used to describe ESUs with the ground measurements.

Column	Var.Name	Comment
1	Plot #	Number of the field plot in the site
2	Plot Label	Label of the plot in the site
3	ESU #	Number of the Elementary Sampling Unit (ESU)
4	ESU Label	Label of the ESU in the campaign
5	Northing Coord.	Geographical coordinate: Latitude (°), WGS-84
6	Easting Coord.	Geographical coordinate: Longitude (°), WGS-84
7	Extent (m) of ESU (diameter)	Size of the ESU ⁽¹⁾
8	Land Cover	Detailed land cover
9	Start Date (dd/mm/yyyy)	Starting date of measurements
10	End Date (dd/mm/yyyy)	Ending date of measurements
11+4*j (*)	LAI	Method
12+4*j (*)		Nb. Replications
13+4*j (*)		PRODUCT
14+4*j (*)		Uncertainty
		Instrument
		Number of Replications
		Methodology
		Standard deviation

*LAI_{eff}, LAI, FAPAR and FCOVER

Figure 8 shows the LAI_{eff} and LAI_{true} measurements by the different land cover types in the two campaigns. In the first campaign, Oat presented the highest LAI value (around 4) and the Maize was the lowest (around 1). In the second campaign, Soybean and Maize showed the highest values of LAI whereas Barley showed the lowest. Measurements over Oat fields are only present during the first campaign, whereas the oat fields were harvested in the second one.

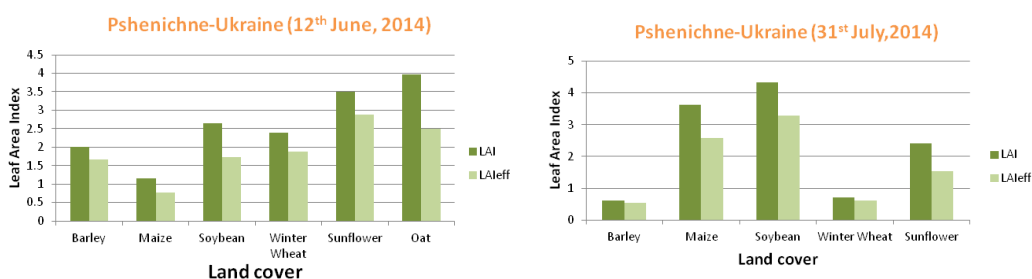


Figure 8: LAI_{eff} and LAI measurements by land cover type over Pshenichne site, Ukraine. Left: 12th June. Right: 31st July.

Figure 9 shows the measurements obtained during the field experiment for the FAPAR as a function of the different land cover types for the two field campaigns. FAPAR values were between 0.4 and 0.9 for the first campaign and between 0.3 and 0.9 for the second. Maize cover presented the minimum value for the first campaign.

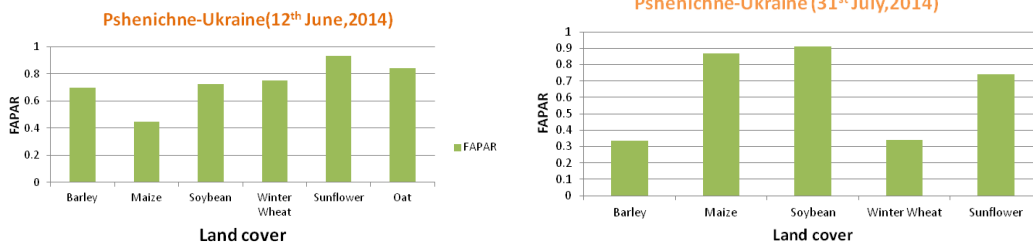


Figure 9: FAPAR measurements by land cover type over Pshenichne site, Ukraine. Left: 12th June. Right: 31st July.

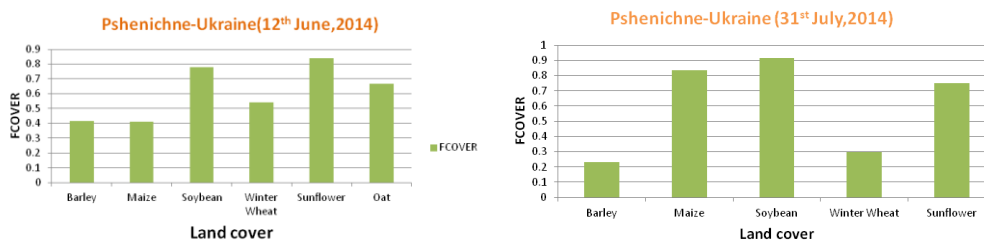


Figure 10: FCOVER measurements by land cover type over Pshenichne site, Ukraine. Left: 12th June. Right: 31st July.

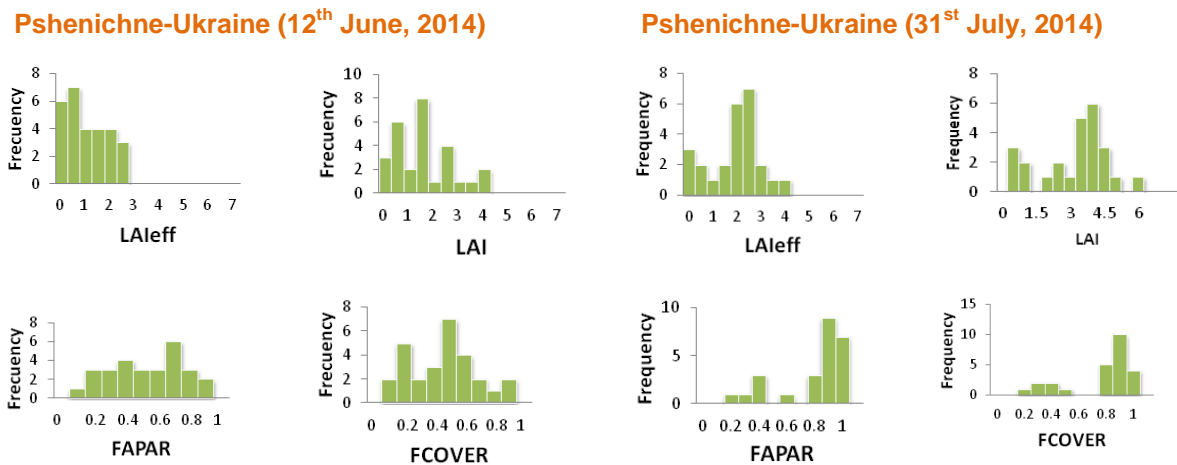


Figure 11: Distribution of the measured biophysical variables. Left side: First campaign. Right side: Second campaign.

Figure 10 shows FCOVER measurements by land cover type for the first and second campaigns. Sunflower and soybean fields presented the highest values of FCOVER during the first campaign. Soybean and maize present values higher for the second one. FCOVER values at the first and second campaign are between 0.4 (barley) to 0.9 (soybean).

Figure 11 shows the distribution of the measured variables, covering typically from medium to high values. However, for the first campaign, the range of LAI is more from low to medium values.

In the first campaign, it can be observed that the frequency values are more homogenous than in the second campaign.

5. EVALUATION OF THE SAMPLING

5.1. EVALUATION BASED ON NDVI VALUES

The sampling strategy is evaluated using the Landsat-8 and Landsat-7 (see Table 5) TOA images by comparing the NDVI distribution over the site with the NDVI distribution over the ESUs. As the number of pixels is drastically different for the ESU and whole site (WS) it is not statistically consistent to directly compare the two NDVI histograms. Therefore, the proposed technique consists in comparing the NDVI cumulative frequency of the two distributions by a Monte-Carlo procedure which aims at comparing the actual frequency to randomly shifted sampling patterns. It consists in:

1. computing the cumulative frequency of the N pixel NDVI that correspond to the exact ESU locations; then, applying a unique random translation to the sampling design (modulo the size of the image)
2. computing the cumulative frequency of NDVI on the randomly shifted sampling design
3. repeating steps 2 and 3, 199 times with 199 different random translation vectors.

This provides a total population of $N = 199 + 1$ (actual) cumulative frequency on which a statistical test at acceptance probability $1 - \alpha = 95\%$ is applied: for a given NDVI level, if the actual ESU density function is between two limits defined by the $N\alpha / 2 = 5$ highest and lowest values of the 200 cumulative frequencies, the hypothesis assuming that WS and ESU NDVI distributions are equivalent is accepted, otherwise it is rejected.

Figure 12 shows that the ESUs NDVI distribution is good over the whole site (comprised between the highest and lowest cumulative frequencies). The sampling presents a small bias towards higher vegetation values, only in the second campaign.

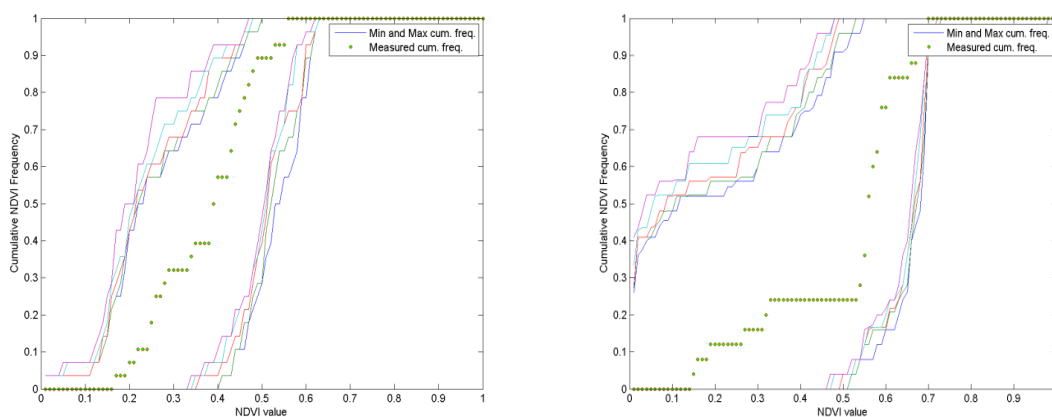


Figure 12: Comparison of NDVI distribution between ESUs and over the whole image, Pshenichne-Ukraine, 2014. Left: 12th June, 2014 Right: 31st July, 2014

5.2. EVALUATION BASED ON CONVEX HULL: PRODUCT QUALITY FLAG.

The interpolation capabilities of the empirical transfer function used for up-scaling the ground data using decametric images is dependent of the sampling (Martinez et al., 2009). A test based on the convex hulls was also carried out to characterize the representativeness of ESUs and the reliability of the empirical transfer function using the different combinations of the selected bands of the Landsat-8 or Landsat-7 TOA images. The result on convex-hulls can be interpreted as:

- pixels inside the 'strict convex-hull': a convex-hull is computed using all the Landsat-8 and Landsat-7 TOA reflectances corresponding to the ESUs belonging to the class. These pixels are well represented by the ground sampling and therefore, when applying a transfer function the degree of confidence in the results will be quite high, since the transfer function will be used as an interpolator;
- pixels inside the 'large convex-hull': a convex-hull is computed using all the reflectance combinations ($\pm 5\%$ in relative value) corresponding to the ESUs. For these pixels, the degree of confidence in the obtained results will be quite good, since the transfer function is used as an extrapolator (but not far from interpolator);
- pixels outside the two convex-hulls: this means that for these pixels, the transfer function will behave as an extrapolator which makes the results less reliable. However, having a priori information on the site may help to evaluate the extrapolation capacities of the transfer function.

Figure 13 shows the results of the Convex-Hull test (i.e., Quality Flag images) for the Pshenichne site over the 5x5 km² study area and the extended 20x20 km² area. For the study area (5x5 km²), the percentage of good interpolation confidence of the transfer function goes up to 77% for the first campaign and 81% for the second campaign (Table 4).

Table 4: Percentages over the two areas over the test site of Pshenichne (Ukraine) Convex hull values: 0=extrapolation of TF, 1=strict convex hull and 2=large convex hull).

Field campaign, 2014	Quality Flags (%)							
	20x20 km ²				5x5 km ²			
DATE	0	1	2	1&2	0	1	2	1&2
Convex hull values	0	1	2	1&2	0	1	2	1&2
12 th June	37%	58%	4%	63%	23%	74%	3%	77%
31 th July	37%	54%	8%	62%	19%	72%	9%	81%

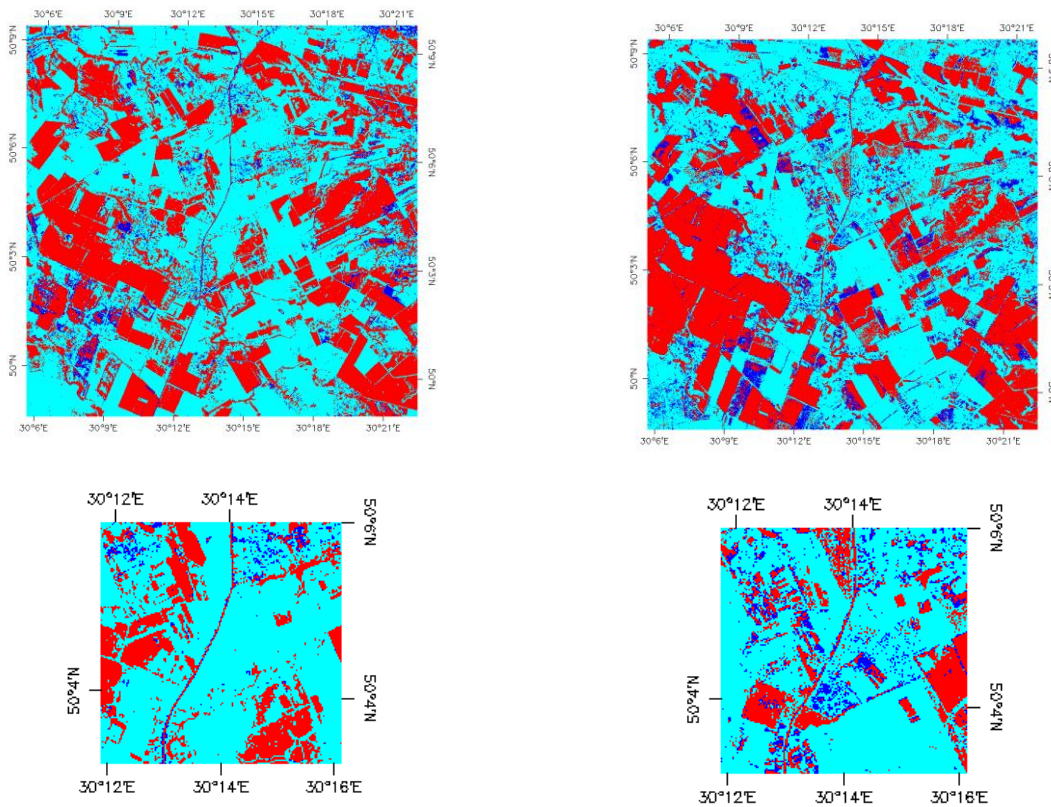


Figure 13: Convex Hull test over 20x20 km² and 5x5 km² areas over Pshenichne site, Ukraine. Left side: 12th June, 2014. Right side: 31st July, 2014. Clear and dark blue correspond to the pixels belonging to the 'strict' and 'large' convex hulls. Red corresponds to the pixels for which the transfer function behaves as extrapolator.

6. PRODUCTION OF GROUND-BASED MAPS

6.1. IMAGERY

The Landsat-8 (OLI) image was acquired the 6th June. As no cloud-free Landsat-8 images was available, for the second campaign Landsat-7 imagery was used instead. The Landsat-7 (ETM+) images were acquired the 1st August 2014 (see Table 5 for acquisition properties). Four spectral bands were selected from 500 nm to 1750 nm with a nadir ground sampling distance of 30 m. The original projection is UTM 36 North, WGS-84.

All Landsat 7 scenes collected since May of 2003 have data gaps. Although the scenes have only 78 percent of their pixels, these data are still some of the most geometrically and radiometrically accurate of all civilian satellite data in the world. A number of methods have been used to fill the gaps of Landsat 7 data. Based on the assumption that the same-class neighboring pixels exhibit similar patterns of spectral differences between dates, we use a simple and effective method to interpolate the values of the pixels within the gaps. This method is the Neighborhood Similar Pixel Interpolator (NSPI). Results indicate that NSPI can restore the value of un-scanned pixels very accurately, and that it works especially well in heterogeneous regions (Chen et al., 2011). Figure 14 shows one example of the good results achieved with the NSPI method. The original Landsat-7 image was corrected using a close Landsat-8 acquisition (12th of June, 2014) to fill the values in the gaps. The result shows very good spatial consistency in the Landsat-7 gap filled image. Figure 15 shows a vertical transect across the image, where all the gaps have been removed in the gap filled image, displaying reliable intra-field variations.

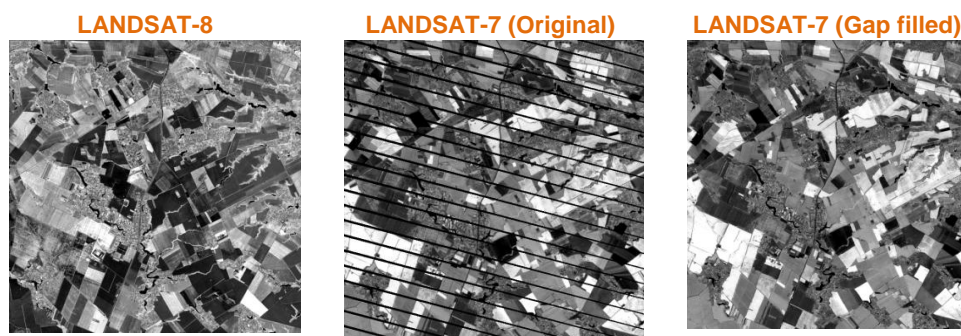


Figure 14: Landsat-8 image for one proximal date (left), the original image Landsat-7 with gaps (middle) and the restored image using the NSPI method (right). Example for NIR bands (B4 for Landsat-7 and B5 for Landsat-8)

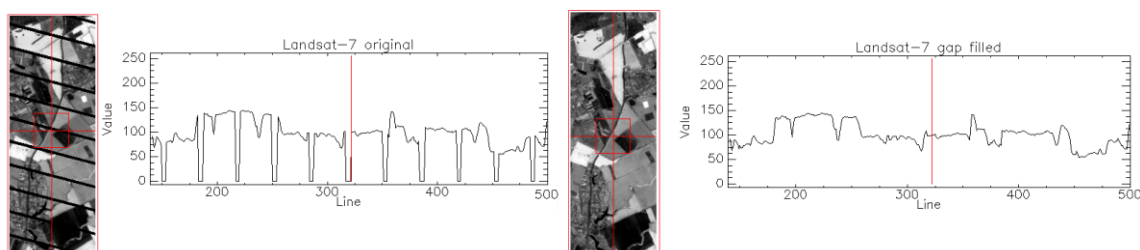


Figure 15: Vertical profile over the Pshenichne site, for NIR band of original Landsat-7 image (Left) and gap filled Landsat-7 image (Right).

Table 5: Acquisition properties of Landsat-8 and Landsat-7 data used for retrieving high resolution maps.

Landsat-8 METADATA		Landsat-7 METADATA	
Platform / Instrument	Landsat-8 / OLI_TIRS	Platform / Instrument	Landsat-7/ETM+
Path	181	Path	181
Row	25	Row	25
Bands	11	Bands	8
Data type	12	Data type	1
Selected spectral range	B3(green) : 0.53-0.59 μm B4(red) : 0.64-0.67 μm B5(NIR) : 0.85-0.88 μm B6(SWIR1) : 1.58-1.65 μm	Selected spectral range	B3(green) : 0.52-0.60 μm B4(red) : 0.63-0.69 μm B5(NIR) : 0.77-0.90 μm B6(SWIR1) : 1.55-1.75 μm
12 th June 2014		31 st July 2014	
Acquisition date	06/06/2014 8:48	Acquisition date	01/08/2014 8:46
Ground control points verify	160	Ground control points verify	169
Geometric RMSE Verify	6.207	Geometric RMSE Verify	4.469
Illumination Azimuth angle	148.40 °	Illumination Azimuth angle	147.69 °
Illumination elevation angle	59.61 °	Illumination elevation angle	54.27 °

6.2. THE TRANSFER FUNCTION

6.2.1. The regression method

If the number of ESUs is enough, multiple robust regression 'REG' between ESUs reflectance and the considered biophysical variable can be applied (Martínez et al., 2009): we used the 'robustfit' function from the Matlab statistics toolbox. It uses an iteratively re-weighted least squares algorithm, with the weights at each iteration computed by applying the bi-square function to the residuals from the previous iteration. This algorithm provides lower weight to ESUs that do not fit well.

The results are less sensitive to outliers in the data as compared with ordinary least squares regression. At the end of the processing, two errors are computed: weighted RMSE (using the weights attributed to each ESU) and cross-validation RMSE (leave-one-out method).

As the method has limited extrapolation capacities, a flag image for each transfer function (Figure 13), are included in the ground based maps in order to inform the users on the reliability of the estimates.

6.2.2. Band combination

Figure 16 show the errors (RW, RC) obtained for the several band combinations using TOA reflectance. The selected combination is: band 1 (green), band 2 (red) band 3 (Near Infrared) and band 4 (Short Wave Infrared) combination. Note that this combination (G, R, NIR, SWIR) was selected for all the variables. These combinations on reflectance were selected since they provide a good compromise between the low cross-validation RMSE, the weighted RMSE (lowest value) and the number of rejected points, but also considering the better sensitivity to the ground measurement.



Figure 16: Test of multiple regression (TF) applied on different band combinations. Band combinations are given in abscissa (1=G, 2=RED, 3=NIR and 4=SWIR). The weighted root mean square error (RMSE) is presented in red along with the cross-validation RMSE in green. The numbers indicate the number of data used for the robust regression with a weight lower than 0.7 that could be considered as outliers. Left side: 12th June, 2014. Right side: 31st July, 2014.

6.2.3. The selected Transfer Function

The applied transfer function is detailed in Table 6, along with its weighted and cross validated errors.

Table 6: Transfer function applied to the whole site for LA_{leff}, LAI, FAPAR daily integrated and FCOVER. RW for weighted RMSE, and RC for cross-validation RMSE

Variable	Band combination	RW	RC
First Campaign			
LA _{leff}	$-0.358-0.00004(\text{SWIR})+0.0002(\text{NIR})-0.0005(\text{R})+0.0004(\text{G})$	0.267	0.286
LAI _{true}	$7.306+0.0002(\text{SWIR})+0.003(\text{NIR})-0.0008(\text{R})-0.0008(\text{G})$	0.523	0.560
FAPAR	$0.092-0.00003(\text{SWIR})+0.00002(\text{NIR})-0.0003(\text{R})+0.0004(\text{G})$	0.099	0.091
FCOVER	$0.283+0.00005(\text{SWIR})-0.000002(\text{NIR})-0.0006(\text{R})+0.0005(\text{G})$	0.137	0.128
Second Campaign			
LA _{leff}	$2.973-0.000003(\text{SWIR})+0.021(\text{NIR})-0.066(\text{R})-0.014(\text{G})$	0.490	0.478
LAI _{true}	$2.975-0.022(\text{SWIR})+0.035(\text{NIR})-0.063(\text{R})-0.002(\text{G})$	0.472	0.713
FAPAR	$1.210-0.005(\text{SWIR})+0.003(\text{NIR})-0.023(\text{R})+0.007(\text{G})$	0.061	0.057
FCOVER	$0.622-0.007(\text{SWIR})+0.005(\text{NIR})-0.017(\text{R})+0.015(\text{G})$	0.087	0.083

Figure 17 shows scatter-plots between ground observations and their corresponding transfer function (TF) estimates for the selected bands combinations. A good correlation is observed for the LA_{leff}, LAI, FAPAR and FCOVER with points distributed along the 1:1 line and no bias, and small scattering. However, for the LAI and LA_{leff}, the transfer function estimates displays some dispersion for high values.

Pshenichne-Ukraine (12th June, 2014) **Pshenichne-Ukraine (31st July, 2014)**

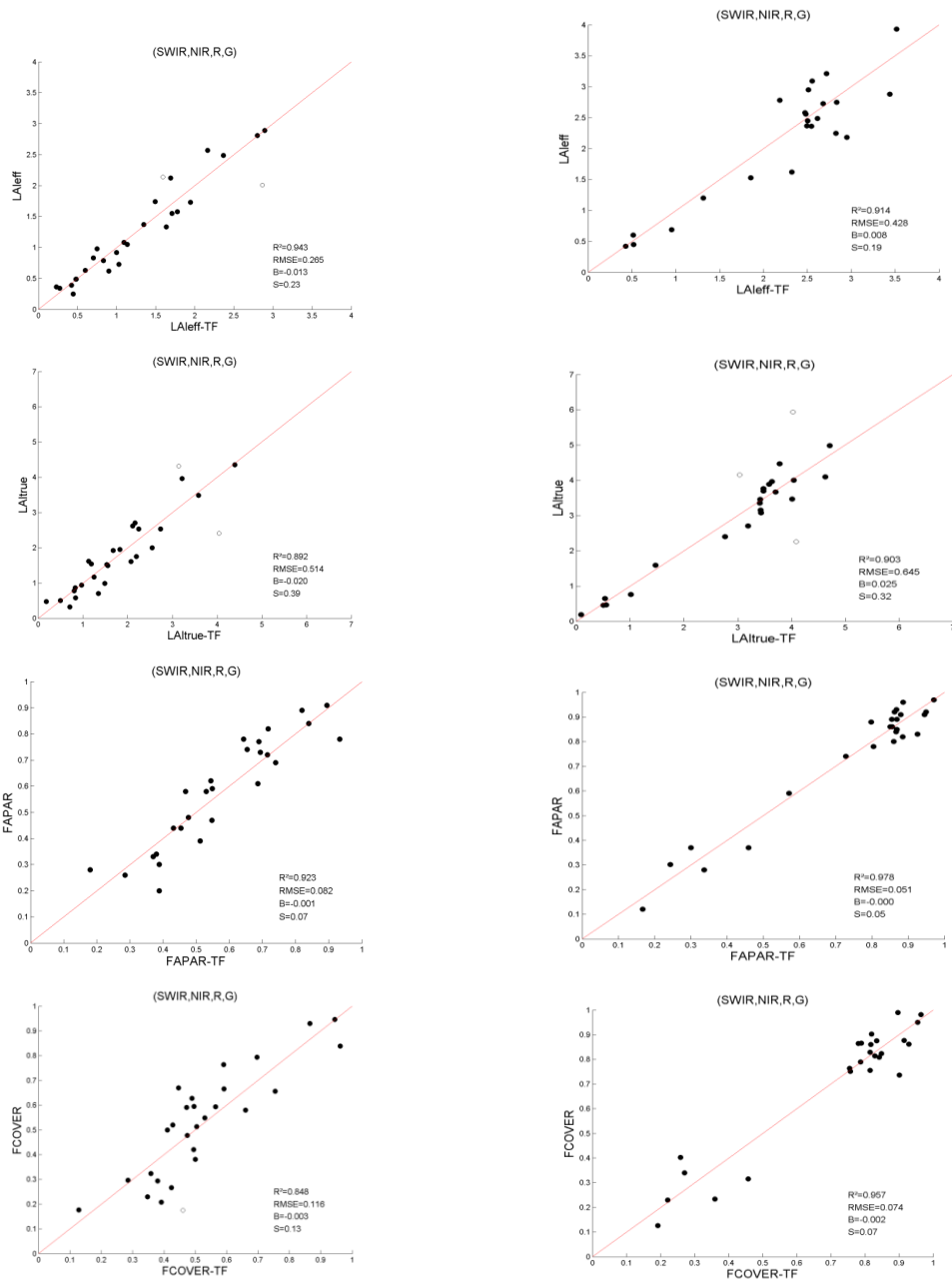


Figure 17: LAI_{eff}, LAI, FAPAR and FCOVER results for regression on reflectance using 4 bands combination. Full dots: Weight>0.7. Empty dots: 0<Weight<0.7.

6.3. THE HIGH RESOLUTION GROUND BASED MAPS

The high resolution maps are obtained applying the selected transfer function (Table 6) to the Landsat-8 or Landsat-7 TOA reflectance. Figure 18, Figure 19, Figure 20, Figure 21 present the TF biophysical maps over the extended 20x20 km² area. Figure 13 shows the Quality Flags included in the final product.

LAI_{eff}

Pshenichne site 12th June, 2014

Pshenichne site 31st July, 2014

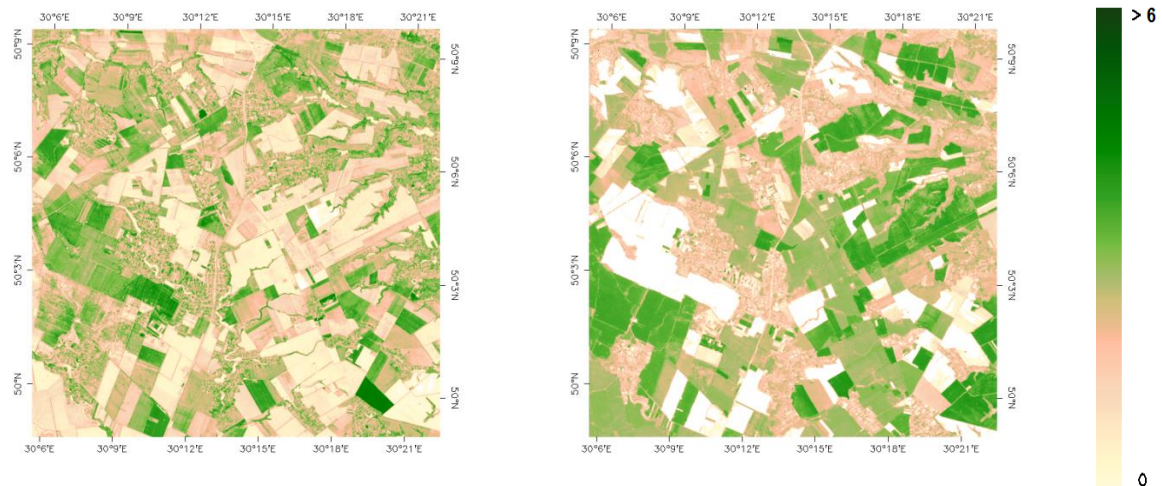


Figure 18: High resolution biophysical LAI_{eff} maps applied on the Pshenichne site. Left: 12th June, 2014. Right: 31st July, 2014.

LAI

Pshenichne site 12th June, 2014

Pshenichne site 31st July, 2014

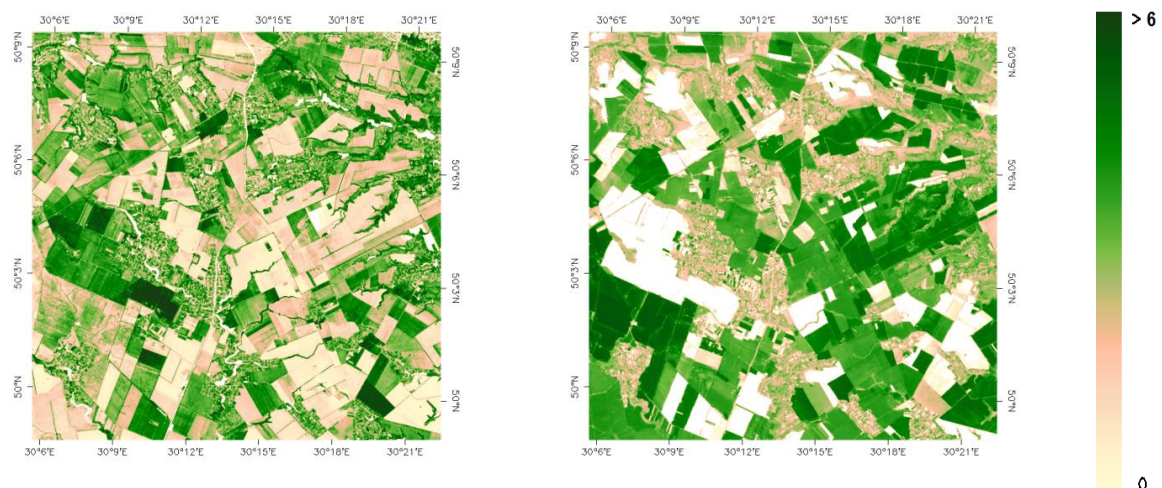


Figure 19: High resolution biophysical LAI maps applied on the Pshenichne site. Left: 12th June, 2014. Right: 31st July, 2014.

FAPAR

Pshenichne site 12th June, 2014

Pshenichne site 31st July, 2014

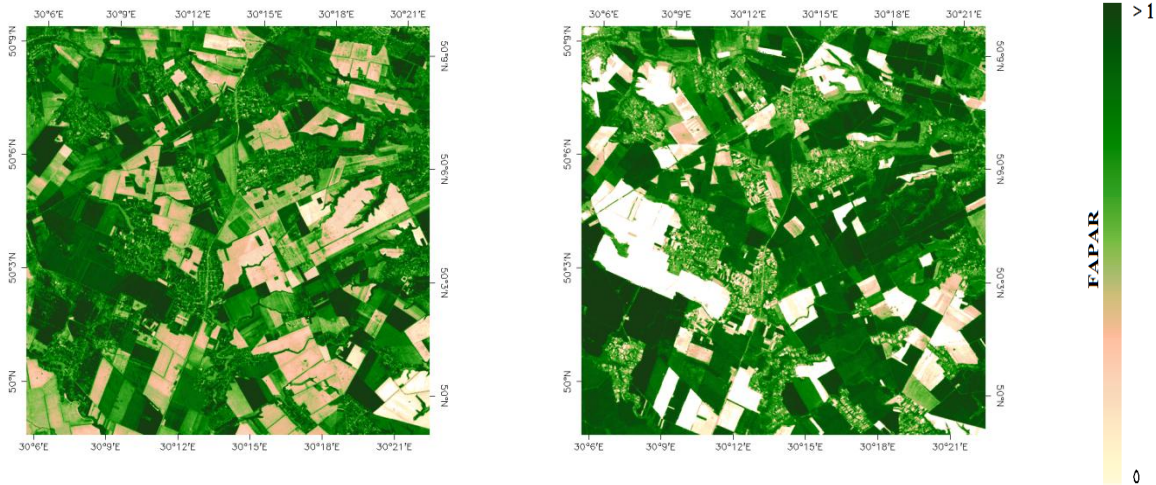


Figure 20: High resolution biophysical FAPAR maps applied on the Pshenichne site. Left: 12th June, 2014. Right: 31st July, 2014.

FCOVER

Pshenichne site 12th June, 2014

Pshenichne site 31st July, 2014

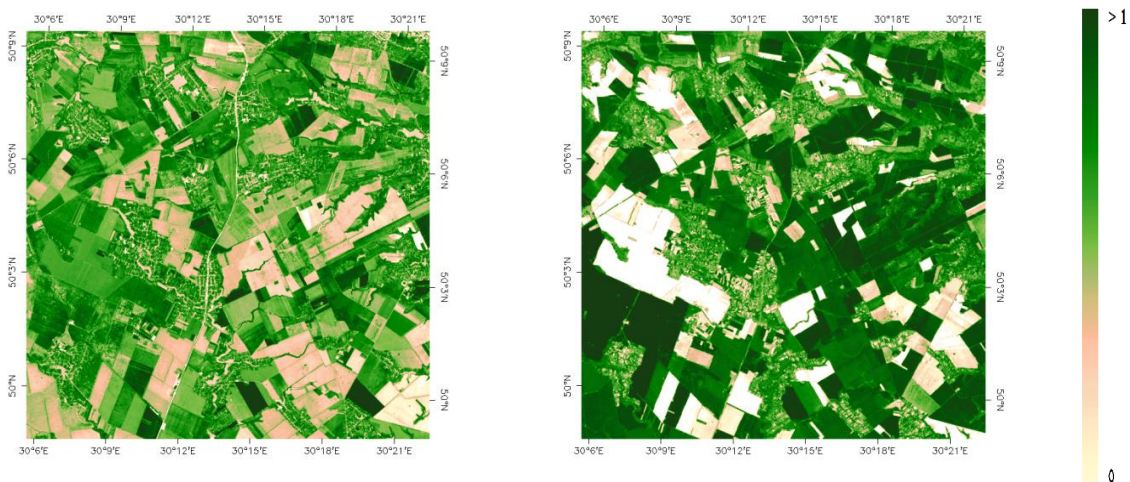


Figure 21: High resolution biophysical FCOVER maps applied on the Pshenichne site. Left: Pshenichne-Ukraine (12th June, 2014). Right: Pshenichne-Ukraine (31st July, 2014).

In the high resolution biophysical maps, we can observe the evolution of the biophysical variables values related to the evolution of the crops between the two campaigns dates. Some fields (e.g. Oat ESU #5) with higher values during the first campaign have been harvested during the second (LAI=FAPAR=FCOVER=0) while other like corn have increased their cover.

Pshenichne site 12th June, 2014

Pshenichne site 31st July, 2014

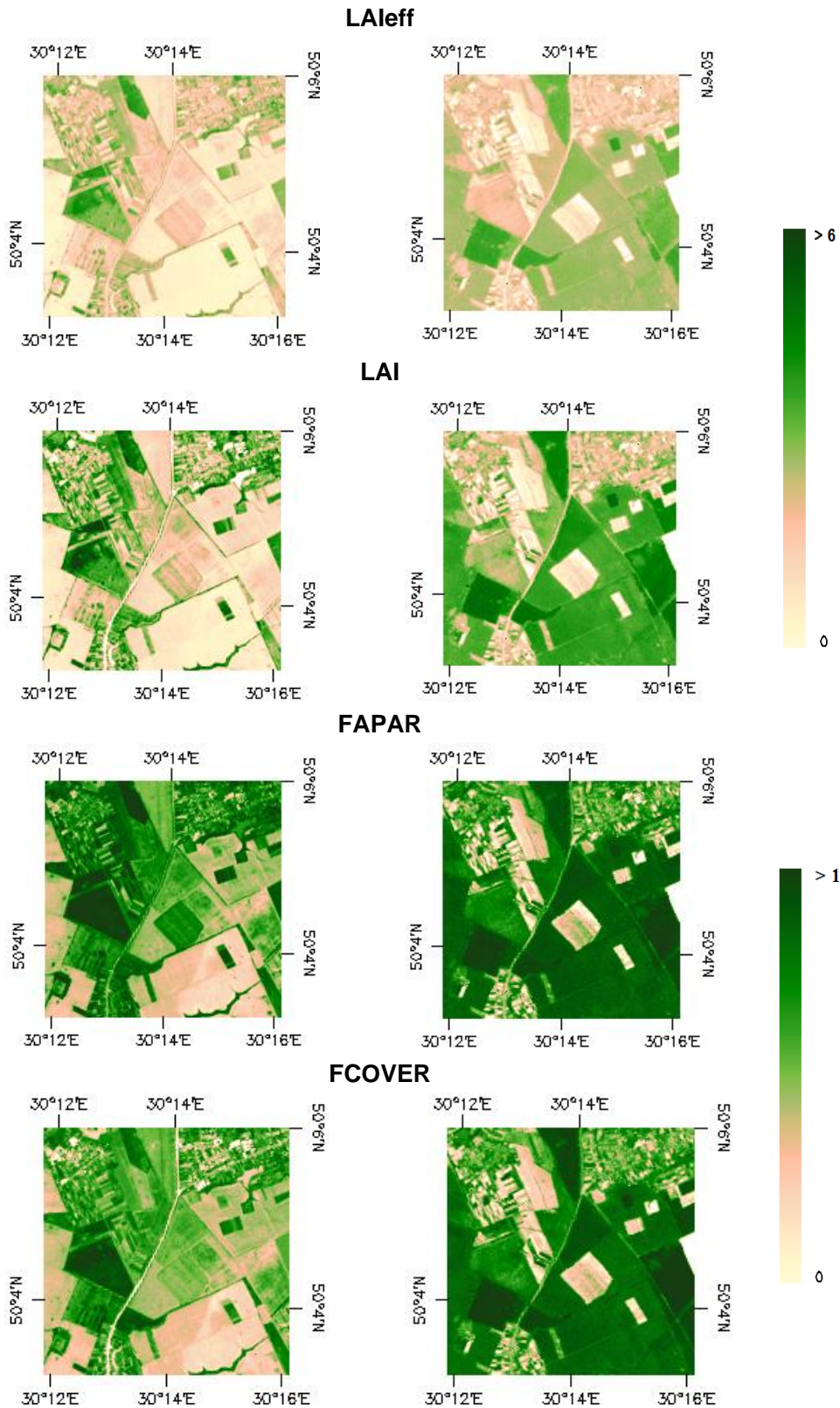


Figure 22: Ground-based maps (5x5 km²) retrieved on the Pshenichne site. Left: First campaign. Right: Second campaign.

Figure 23 shows several scatter plots between biophysical variables that prove the good consistency of the ground-based maps, showing the exponential (LAI vs FAPAR) and linear (FAPAR vs FCOVER) trend observed with the ground data. Note that some scattering is observed between the FAPAR and FCOVER for the first campaign as previously reported for the ground data (Figure 6).

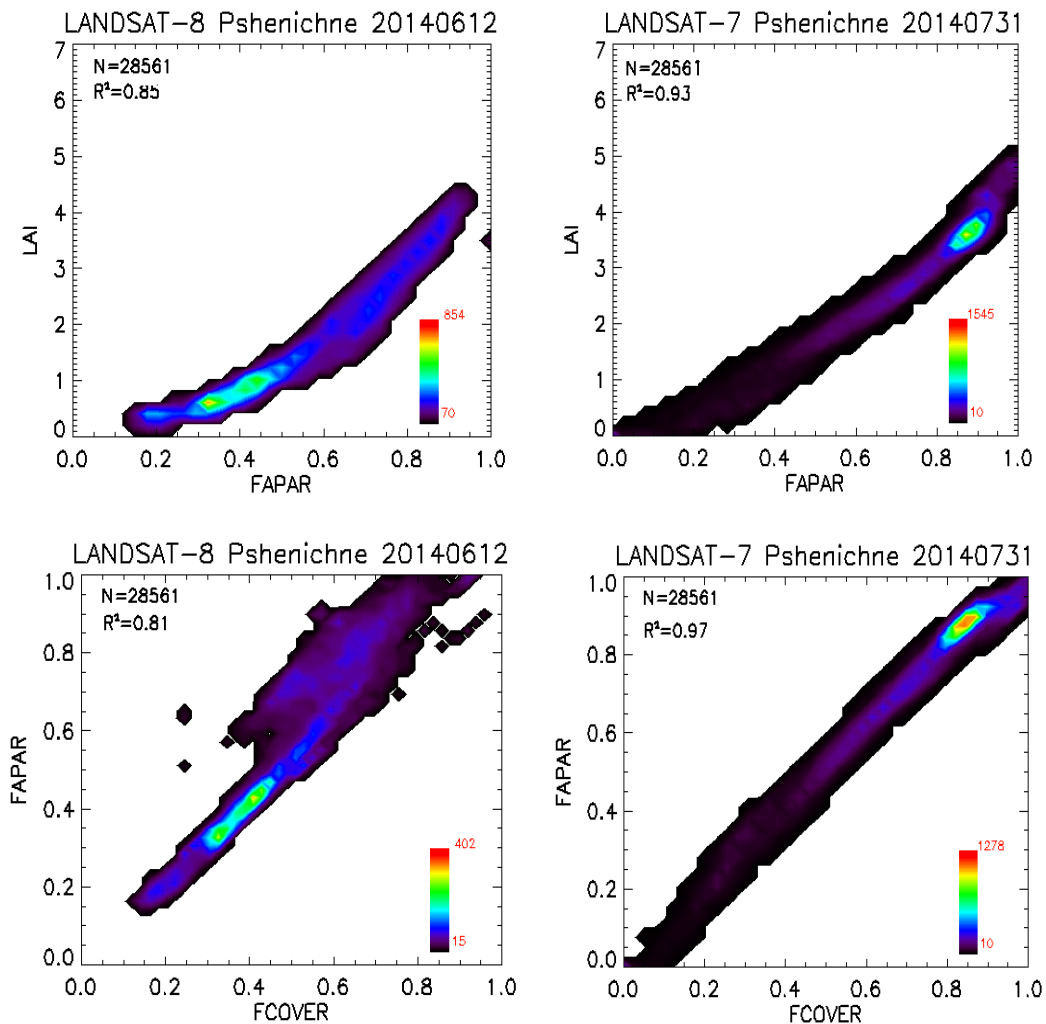


Figure 23: Scatter plots to LAI vs FAPAR and FAPAR vs FCOVER for the two campaigns over Pshenichne-Ukraine. Right: 12th June, 2014. Left: 31st July, 2014.

6.3.1. Mean Values

Mean values of a 3x3 km² area centred in the test site are provided for validation of 1 km satellite products to reduce co-registration and PSF errors, and in agreement with the CEOS OLIVE direct dataset (Table 7). For the validation of coarser resolutions product (e.g. MSG products) a larger area should be considered. For this reason empirical maps are provided at 5x5 km², and 20x20 km².

Table 7: Mean values and standard deviation (STD) of the HR biophysical maps for the selected 3 x 3 km² area at Pshenichne site (Ukraine)

Pshenichne	LATITUDE		LONGITUDE	
	50.07653760° N		30.23226820° E	
	First campaign (June)		Second campaign (July)	
	MEAN	STD	MEAN	STD
LAI _{eff}	1.55	0.87	2.01	0.92
LAI _{true}	2.14	1.19	2.76	1.29
FAPAR daily	0.64	0.21	0.7	0.25
FCOVER	0.55	0.19	0.68	0.24

Table 8 describes the content of the geo-biophysical maps in the nomenclature: "BIO_YYYYMMDD_SENSOR_Site_ETF_Area"

where:

BIO stands for Biophysical (LAI_{eff}, LAI, FAPAR and FCOVER)

SENSOR = LANDSAT8 or LANDSAT7

YYYYMMDD = Acquisition date

Site = Pshenichne

ETF stands for Empirical Transfer Function

Area = 20x20 and 5x5

Table 8: Content of the dataset.

Parameter	Dataset name	Range	Variable Type	Scale Factor	No Value
LAI effective	LAI _{eff}	[0, 7]	Integer	1000	-1
LAI	LAI	[0, 7]	Integer	1000	-1
FAPAR (Daily)	FAPAR	[0, 1]	Integer	10000	-1
Fraction of Vegetation Cover	FCOVER	[0, 1]	Integer	10000	-1
Quality Flag	QFlag	0,1,2 (*)	Integer	N/A	-1

(*) 0 means extrapolated value (low confidence), 1 strict interpolator (best confidence), 2 large interpolator (medium confidence)

7. CONCLUSIONS

The FP7 ImagineS project continues the innovation and development activities to support the operations of the Copernicus Global Land service. One of the ImagineS demonstration sites is located near Pshenichne, in the Province of Kiev, in Ukraine.

This report presents the ground data collected during two intensive field campaigns: 12th of June and 31th of July 2014. The dataset includes 28 and 25 elementary sampling units, respectively, where digital hemispherical photographs were taken and processed with the CAN-EYE software to provide LAI, LAI_{eff}, FAPAR and FCOVER values to characterize the cultivated vegetation of the area: barley, maize, soybean, winter wheat, sunflower and, only in the first campaign, oat.

High resolution ground-based maps of the biophysical variables were produced over the site. Ground-based maps have been derived using high resolution imagery (Landsat-8 TOA in the first campaign and Landsat-7 TOA in the second campaign) according with the CEOS LPV recommendations for validation of low resolution satellite sensors. Transfer functions have been derived by multiple robust regressions between ESUs reflectance and the several biophysical variables. The spectral band combinations to minimize errors (weighted RMSE and cross-validation RMSE) were band 1 (green), band 2 (red), band 3 (Near Infrared) and band 4 (Short Wave Infrared) combination, for the two campaigns. The RMSE values for the transfer function estimates are ranging between 0.27 and 0.43 for LAI_{eff}, 0.51 and 0.65 for LAI, 0.08 and 0.05 for daily integrated FAPAR, and finally 0.12 and 0.07 for FCOVER, with no bias.

The quality flag maps based on the convex-hull analysis show very good quality around the study area. The percentages for the transfer functions of good interpolation capabilities for the 5x5 km² study area are 77% and 81% for the first and the second campaigns, respectively.

The biophysical variable maps are available in geographic (UTM 32 North projection WGS-84) coordinates at 30 m resolution over the 20x20 km² and 5x5 km² over the site. Mean values and standard deviation over a validation area of 3x3 km² for LAI_{eff}, LAI, FCOVER and FAPAR were computed centered at the validation test site.

8. ACKNOWLEDGEMENTS

This study is supported by the FP7 IMAGINES project under Grant Agreement N°311766. Landsat 8 and Landsat 7 imagery are provided through the USGS Global Visualization service. This work is done in collaboration with the consortium implementing the Global Component of the Copernicus Land Service.

Thanks to the Space Research Institute NAS Ukraine and SSA for providing the field data.

9. REFERENCES

- Baret, F. and Fernandes, R. (2012). Validation Concept. VALSE2-PR-014-INRA, 42 pp.
- Camacho, F., Cernicharo, J., Lacaze, R., Baret, F., and Weiss, M. (2013). GEOV1: LAI, FAPAR Essential Climate Variables and FCOVER global time series capitalizing over existing products. Part 2: Validation and intercomparison with reference products. *Remote Sensing of Environment*, 137: 310-329.
- Chen, J., Zhu X., Vogelmann J. E., Gao F., Jin S. (2011). A simple and effective method for filling gaps in Landsat ETM+ SLC-off images. *Remote sensing of environment*. 115: 1053-1064.
- Demarez, V., Duthoit, S., Baret, F., Weiss, M. and Dedieu, G. (2008). Estimation of leaf area and clumping indexes of crops with hemispherical photographs. *Agricultural and Forest Meteorology*. 148, 644-655.
- Fernandes, R., Plummer, S., Nightingale, J., et al. (2014). Global Leaf Area Index Product Validation Good Practices. CEOS Working Group on Calibration and Validation - Land Product Validation Sub-Group. *Version 2.0: Public version made available on LPV website*.
- Martínez, B., García-Haro, F. J., & Camacho, F. (2009). Derivation of high-resolution leaf area index maps in support of validation activities: Application to the cropland Barrax site. *Agricultural and Forest Meteorology*, 149, 130–145.
- Miller, J.B. (1967). A formula for average foliage density. *Aust. J. Bot.*, 15:141-144
- Morissette, J. T., Baret, F., Privette, J. L., Myneni, R. B., Nickeson, J. E., Garrigues, S., et al. (2006). Validation of global moderate-resolution LAI products: A framework proposed within the CEOS land product validation subgroup. *IEEE Transactions on Geoscience and Remote Sensing*, 44, 1804–1817.
- Latorre, C., Camacho, F., Sánchez, J., Kussul, N., Serhiy, S., Kravchenko, O., (2013). "Vegetation Field Data and Production of Ground-Based Maps: 14th May, 15th June and 15th July. Pshenichne site, Ukraine" report. (Available at ImagineS website: <http://fp7-imagines.eu/pages/documents.php>).
- Weiss, M., Baret, F., Smith, G.J., Jonckheere, I. and Coppin, P., (2004). Review of methods for in situ leaf area index (LAI) determination. Part II. Estimation of LAI, errors and sampling. *Agricultural and Forest Meteorology*. 121, 37–53.
- Weiss M. and Baret F. (2010). CAN-EYE V6.1 User Manual
- Welles, J.M. and Norman, J.M., 1991. Instrument for indirect measurement of canopy architecture. *Agronomy J.*, 83(5): 818-825.